Journal of Thermal Analysis and Calorimetry, Vol. 69 (2002) 23–36

ANALYSIS OF THE ENERGETIC HETEROGENITY OF $HgBa_2Ca_2Cu_3O_{8+\delta}$ SURFACES Q-TG and Q-DTG data

P. Staszczuk[1]*, D. Sternik*[1] *and V. V. Kutarov*[2]

[1]Department of Physicochemistry of Solid Surface, Chemistry Faculty, Maria Curie-Skłodowska University, M. Curie-Skłodowska Sq. 3, 20-031 Lublin, Poland
[2]Physical Research Institute, Odessa University, Pastera Str. 27, Odessa 270026, Ukraine

Abstract

Energetic heterogeneity of adsorbents is conditioned by the differences in topology of adsorption centres, dispersion of pore sizes and other factors. This paper describes theoretical and experimental studies that demonstrate a method for estimation of the energetic heterogeneity of adsorbents by making use of the results from single thermogravimetry Q-TG and Q-DTG curves, recorded under quasi-equilibrium conditions, for preadsorbed liquid on a porous solid surface.

Keywords: energetic heterogeneity, $HgBa_2Ca_2Cu_3O_{8+\delta}$, quasi-isothermal thermogravimetry, thermodesorption of liquid

Introduction

In relation to energies, surfaces can be divided into two types: homogeneous and heterogeneous [1, 2]. These surface areas possess different energetic minimum depending on the type, thus different adsorption energies, ΔE°, and different potential barriers for surface diffusion, ΔV°. For ideally homogeneous surfaces ΔE°=constant (Fig. 1a) but, in practice, we have the situations presented in Fig. 1b.

There are two cases:

(i) when $kT>\Delta V^{\circ}$ – mobile adsorption and molecules can move along the surfaces,

(ii) when $kT<\Delta V^{\circ}$ – localized adsorption with strong localization of molecules in the minimum.

For heterogeneous surfaces: in this case it is characteristic that the minimum have different depths on a single surface, so different energetic barriers for diffusion exist. Heterogeneous surfaces are divided, in relation to the minimum, into:

i/ Periodic heterogeneous surfaces where the energetic minima exhibit some reproducibility which can be represented as in Fig. 2a.

ii/ Completely random, where the minima do not exhibit any reproducibility (Fig. 2b).

1418–2874/2002/ $ 5.00

Akadémiai Kiadó, Budapest
Kluwer Academic Publishers, Dordrecht

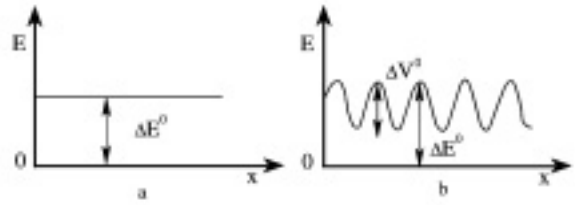

Fig. 1 Dependence of adsorption energy on distances from the surface (homogenous surface)

iii/ Patchwise, where some reproducibility of energetic minima occurs they are grouped in large patches which can be represented in as in Fig. 2c.

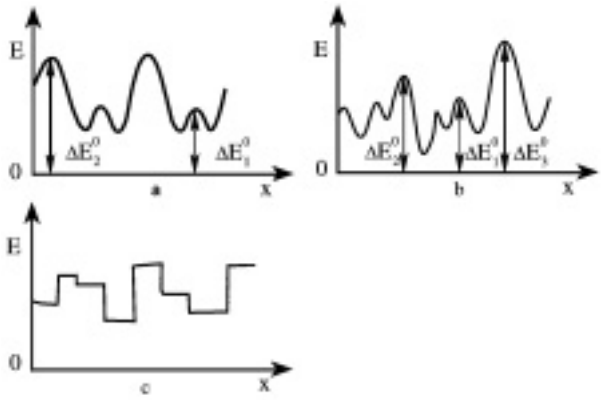

Fig. 2 Dependence of adsorption energy on distances from the surface (heterogeneous surface)

Of the above mentioned types of heterogeneous surfaces, two extreme topographic models are of greater importance, because they are employed for describing most phenomena concerning adsorption on solid surfaces. These are the patchwise (or 'homotattic') type surfaces where sites of equal adsorption energy are assumed to be grouped into patches and the random type surfaces where adsorption sites with different adsorption energies are distributed over the surface completely at random [2]. It is usually assumed that patches are so large that, in practice, they constitute independent adsorption (thermodymanic) centers which are only in thermal and material contact (model considered by Ross and Olivier [3]). Adsorbate molecule exchange is possible between these subsystems. It is assumed that the system states in which two interacting molecules are adsorbed on two different patches make negligible contributions to the thermodynamic properties of the systems.

This is presented in Fig. 3a. The random type of surface topography is illustrated in Fig. 3b. Such a completely random distribution of centers causes the probability of finding another center in the neighbourhood of any adsorption center to be identical (model introduced by Hill [4]). As a result, the microscopic composition of the phase adsorbed in the neighbourhood of any centre is the same and identical to the mean

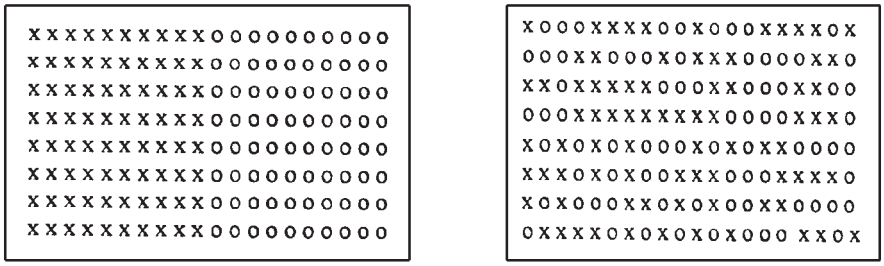

a b

Fig. 3 The scheme of surface topography: a – patches and b – random type

composition of the phase on the whole solid surface. In the first case (the patchwise one) there is an observed high correlation between adsorption energies, i.e. the energies change on passing into other adsorption centers, but the difference remains unchanged. In the second case (the random case) no correlation is observed between adsorption energies on different centers.

Real systems have properties intermediate between these extreme physical situations. It can be assumed that in the case of well-formed crystals with a few crystallographic planes, the patchwise model application is more justifiable. The random model better describes amorphous samples. Even in the case of well-formed crystals, that are the samples of very high degree of the oxide bulk arrangement, the surface may have a small degree of surface atoms arrangement. The strategy of the present investigations consists in the analysis of the properties of different extreme models and identification of the model that best describes the experimental system under consideration.

The numerical procedure was developed in order to determine the desorption energy distribution functions (i.e. total heterogeneity) of a preadsorped liquid on a mesoporous solid surface from single thermogravimetry Q-DTG curve recorded under quasi-equilibrium conditions [5]. The procedure is based on the application of a condensation approximation to treat the desorption kinetics under non-isothermal conditions. In this approximation, the desorption energy at each temperature in the Q-DTG curve was calculated using Redhead's equation [6]. The desorption distribution was calculated from the first derivative of the temperature on the desorption energy, E_d. The pore-size and the desorption energy are a function of the vaporization heat for the test liquid its, molar volume and surface tension. The mesopore-size cumulative and differential distributions can be evaluated from the dependence of the desorption energy versus mesopore volume, V_{pore}, and above desorption distribution, respectively. The approximate desorption energy distribution from the pores for each temperature T_i in the Q-DTG curve is given by the equation: $\rho(E_d) = -(V_{pore}/dT_i)(dT_i/dE_d)$.

It was stated during our last investigations that the number, intensity and shape of Q-DTG curves reflect the effects of the desorption energy distribution functions of the $HgBa_2Ca_2Cu_3O_{8+\delta}$ surface and is typical for those of the $HgBa_2Ca_2Cu_3O_{8+\delta}$ measured by independent methods. The present study demonstrates the possibility to use

the single Q-TG and Q-DTG curve for the quantitative characterization of the total energetic heterogeneity of the nonporous and porous surfaces.

Theory

The energetic heterogeneity of adsorbents is conditioned by the differences in topology of adsorption centres, dispersion of pore sizes and other factors. This paper describes a method for the estimation of the energetic heterogeneity of sorbents makes that use of the results of the programmed thermodesorption of liquids from the solid surface.

In the case of non-associated, one-component layers, the kinetics of monomolecular desorption described by the following equation [7, 8]:

$$-\frac{\mathrm{d}\theta}{\mathrm{d}t}=\nu(1-\theta)\exp\left(-\frac{E}{RT}\right) \tag{1}$$

where $T=T_o+\beta t$, θ – the degree of surface coverage, ν – the entropy factor, E – the desorption energy, T_o, T – the initial and given temperatures of desorption, β – the sample heating rate, t – the time.

Equation (1) holds true when the amount of desorbed substance does not cover the whole surface area uniformly and the basic desorption process takes place in the range of capillary condensation. Equation (1) can also be used for the analysis of desorption from an energetically heterogeneous, multilayer covered solid surface. In this case, the desorption rate is described by the integral equation [9, 10]:

$$-\frac{\mathrm{d}\theta}{\mathrm{d}T}=\int_{\mathrm{E}}\varphi(E)(1-\theta)\frac{\nu}{\beta}\exp\left(-\frac{E}{RT}\right)\mathrm{d}E \tag{2}$$

Equation (2) – is the 1st degree Fredholm integral equation [2]. In Eq. (2) the element of integration can be determined as:

$$Z(E)=(1-\theta)\frac{\nu}{\beta}\exp\left(-\frac{E}{RT}\right) \tag{3}$$

The energetic heterogeneity of the sorbent surface is described using the distribution function $\varphi(E)$, i.e. probability distribution of adsorption centres on the surface in relation to the magnitude of the desorption energy. In order to determine the distribution function $\varphi(E)$ it is necessary to solve the integral Eq. (2). Accurate ways of solving the integral Eq. (2) analytically are possible only when the analytical expression for the left side of Eq. (2) is known. Since such information does not exist apriori, successful application of exact analytical methods of solving Eq. (2) proves difficult. Moreover, a complicated form of the $Z(E)$ expression in Eq. (2) makes it impossible to solve the energy distribution function $\varphi(E)$ in a simple way.

In fact, for an analytical solution of Eq. (2), the exact expression $Z(E)$ can be substituted by an approximate expression and a new approximate integral equation can be solved. However, application of the approximate integral expression in Eq. (2) means neglecting application of the kinetic desorption equation and increasing the

probability of error in the estimation of the quantity $\varphi_n(E)$. Therefore, determination of the distribution function $\varphi_n(E)$ is made by means of numerical methods [9].

The shape of the element of integration function (3) can be analysed using the analytical method [11]. According to this method, the equation of desorption kinetics (1) for the part of surface characterised by a constant value of desorption energy has the form [11]:

$$-\frac{1}{1-\theta_i}\frac{d\theta_i}{dT}=\frac{\nu_i}{\beta}\exp\left(-\frac{E_i}{RT}\right) \tag{4}$$

The general form of the desorption kinetics is given in the following equation [11]:

$$-\frac{1}{1-\theta}\frac{d\theta}{dT}=\sum_{i=1}^{\infty}\frac{\nu_i}{\beta}\exp\left(-\frac{E}{RT}\right) \tag{5}$$

and, after transformation:

$$\ln\left[-\frac{1}{(1-\theta)}\frac{d\theta}{dT}\right]=f\left(\frac{1}{T}\right) \tag{6}$$

Using function (6) for contingence and numerical differentiation methods, it is possible to determine some discrete quantities of the desorption energy E, entropy coefficient ν and dependence $\theta(E)$ [11]. Dependence of quantity θ on desorption energy, E, can be expressed in linear, exponential or hyperbolic dependence forms. For the desorption spectrum, differences in interaction energies are not significant. Their size diminishes with an increase of desorption energy. One can assume that, for each individual peak, the dependence of the quantity θ on desorption energy can be expressed by means of the linear function:

$$\theta=AE-B \tag{7}$$

The validity of using function (7) was confirmed in paper [6]. Dependence of entropy coefficient, ν, on desorption energy, E, is expressed by means of the exponential function [12–15]:

$$\nu=n\exp(mE) \tag{8}$$

Then Eq. (2) taking into account dependences (7) and (8) can be written as follows:

$$-\frac{d\theta}{dT}=\int_E \varphi(E)(1+B-AE)n e^{-\frac{(1-m)E}{RT}}dE \tag{9}$$

where m, n – constants.

Let us consider the properties of the element of integration function of Eq. (9). For thermodesorption of organic substances from the surface of such sorbents as zeolites, active carbon or metal oxides, the characteristic range of desorption temperatures is 50–220°C. However, for desorption from meso- and micropores, the temperature range decreases to 100–220°C and the desorption energies, E=30–80 kJ mol^{-1}

[6] correspond to this temperature range. The greatest energetic heterogeneity of the surface of the above mentioned materials is characteristic just for mesopores. The temperature and desorption energy ranges make it possible to assume that the element of integration function has a sharp maximum which determines the desorption rate for a given value of E/RT. It can be also assumed that the function $\varphi(E)$ is continuous and changes slowly. Assuming that, in a small range of the element of integration expression maximum, Eq. (9) can be written in the following way [16]:

$$-\frac{\mathrm{d}\theta}{\mathrm{d}T}=n\varphi(E)\int_{\mathrm{E}}(1+b-AE)\mathrm{e}^{-\frac{(1-\mathrm{m})\mathrm{E}}{\mathrm{RT}}}\mathrm{d}E \tag{10}$$

After its solution there is obtained the equation:

$$-\frac{\mathrm{d}\theta}{\mathrm{d}T}=\frac{nRt}{(1-m)}\varphi(E)N \tag{11}$$

where $N=\left|_{E_{\min}}^{E_{\max}}\right\{-(1+B)\mathrm{e}^{-\frac{(1-\mathrm{m})\mathrm{E}}{\mathrm{RT}}}-A\mathrm{e}^{-\frac{(1-\mathrm{m})\mathrm{E}}{\mathrm{RT}}}\left[\frac{(1-m)}{RT}E+1\right]\right\}$.

The final expression for determination of the desorption energy distribution function has the form:

$$\varphi(E)=-\frac{\mathrm{d}\theta}{\mathrm{d}T}\frac{(1-m)}{nR+N} \tag{12}$$

The real form of the distribution function $\varphi_n(E)$ is obtained by normalization of the function $\varphi(E)$:

$$\varphi_{\mathrm{n}}(E)=\frac{\varphi(E)}{\int_{\mathrm{E}}\varphi(E)\mathrm{d}E} \tag{13}$$

For the correctly calculated distribution function of the desorption energy, the equation should satisfy the normalisation conditions:

$$\int_{\mathrm{E}}\varphi_{\mathrm{n}}(E)\mathrm{d}E=1 \tag{14}$$

After calculating the normalised density function, $\varphi_n(E)$, according to Eq. (12), all size constants reduce reciprocally which makes calculation of the quantity $\varphi_n(E)$ much easier:

$$\varphi_{\mathrm{n}}(E)=-\frac{\mathrm{d}\theta}{\mathrm{d}T}\frac{1}{T} \tag{15}$$

For the calculation to which there has been applied the numerical differentiation procedure [14]:

$$\varphi(E)=\frac{\theta_{i+1}-\theta_i}{E_{i+1}-E_i} \tag{16}$$

This paper presents the studies of energetic heterogeneity on the basis of *n*-octane desorption from the surface of a high-temperature superconductor $HgBa_2Ca_2Cu_3O_{8+\delta}$ (so-called Hg-1223) from Q-TG and Q-DTG data.

Experimental

Materials

Since the discovery of superconductivity in compounds Hg-1223 [24] in 1993 there has been a great development of theoretical and experimental studies to investigate and explain the mechanism of superconductivity in these compounds.

This compound presented in Fig. 4 belongs to the homologous series of compounds including mercury as the basis for superconductive oxides of the general formula $HgBa_2Ca_{(n-1)}Cu_nO_y$ (n=1, 2, 3). The structure of these compounds is based on the following layers:

$$....[(BaO)_c(HgO_\delta)_o(BaO)_c(CuO_2)_o$$
$$\{(n-1)(Ca)_c(CuO_2)_o\}](BaO)_c....$$

in which the group $(BaO)_c(HgOd_\delta)_o(BaO)_c$ has the salt structure but the group $(CuO_2)_o\{(n-1)(Ca)_c(CuO_2)_o\}$ has the structure similar to peroskovite [19, 20]. In the case of Hg-1223 there are two kinds of (CuO_2) layers, one in which the copper atom has five-fold pyramidal coordination, and one in which the copper coordination is square planar [19]. This material belongs to the group of high-temperature superconductors of the critical temperature T_c=133.5 K [18–22] and at high pressures T_c=~150 K [23]. This is a non-porous adsorbent with the specific surface area calculated from the BET adsorption isotherm of 0.89 $m^2\ g^{-1}$ [25]. A description of its physical properties can be found in paper [24] and that of sorption properties in [25].

Method

The Hg-1223 sample was typically dried at 200°C. The thickness of adsorbed liquid layers on the surface can be controlled by the immersion mode of the solid sample. The immersion of a sample in *n*-octane vapours in a vacuum dessicator, where p/p_0=1, blocks all adsorption active centers, the surface and capillary forces of the sample studied [26]. The studies were made using a simultaneous derivatograph Q-1500 D (MOM, Budapest, Hungary) [27]. The thermodesorption of *n*-octane measurements was carried out in quasi-isothermal condition, in static air, in a temperature range of 20–250°C with a furnance heating rate of 6°C min^{-1}. The Q-TG and Q-DTG curves were registered digitally under the control of the program Derivat running on a PC. The series of 3 experiments of *n*-octane thermodesorption from sample studied have been made and average data were used in our calculations.

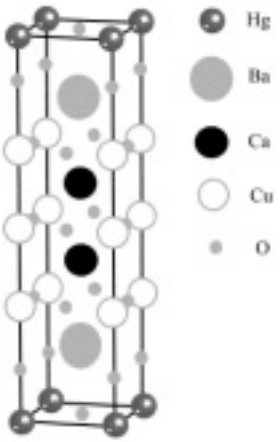

Fig. 4 The schematic structure of Hg-1223

Results and discussion

Figure 5 presents the experimental differential curve Q-DTG depending on temperature for the thermodesorption of a *n*-octane film from the surface of $HgBa_2Ca_2Cu_3O_{8+\delta}$. While analyzing the curve Q-DTG it is possible to distinguish four stages of thermodesorption: the first large peak in the temperature range T=110–140°C corresponding to desorption of *n*-octane from mesopores and the successive peaks in the temperature ranges: II – T=140–160°C, III – T=160–170°C and IV – T=170–180°C connected with desorption from micropores and various active centres of the surface. The appearance of several peaks results from the non-linear dependence of the adsorption energy on the degree of coverage θ (Eq. (3)) as well as from lateral interactions between adsorbed liquid molecules. Reciprocal lateral interactions lead to the increase of desorption temperature range and width of the Q-DTG peak. Figure 6 presents a graphical form of Eq. (5) for *n*-octane thermodesorption from the sample surface. A large degree of non-linearity dependence (Eq. (6)) shown in Fig. 6 indicates the large energetic heterogeneity of the superconductive material under consideration. Using the contingence method for the curve in Fig. 6, or the numerical differentiation method, the dependence of the degree of coverage, θ(E), as a function of desorption energy E_d, is presented in Fig. 7. The distribution function of the desorption energy of *n*-octane from the surface of the studied sample is presented in Fig. 8 for the whole temperature range 50–180°C.

The desorption energy calculated in the whole temperature range changes from 28 to 60 kJ mol^{-1}. Calculations of the distribution functions $\varphi_n(E)$ for each temperature range mentioned above were made using Eq. (15). It should be stressed that the non-dimensional quantity N in Eq. (12) is a characteristic feature of the non-linearity of the desorption energy change for each stage I–IV. The quantity N calculated for the above mentioned ranges is: –95, –10, –1.3, –1.1 respectively. The distribution func-

tions $\varphi_n(E)$ for each temperature range I, II, IV are presented in Figs 9–11, respectively. The desorption energy changes from 28 to 48 kJ mol^{-1} in the range 110–140°C (Fig. 9), 50–56 kJ mol^{-1} for the range 140–160°C (Fig. 10) and 60–65 kJ mol^{-1} for the range 170–180°C (Fig. 11). The increase of desorption energy at higher and higher temperatures corresponds to removal of *n*-octane molecules of more strongly bonded

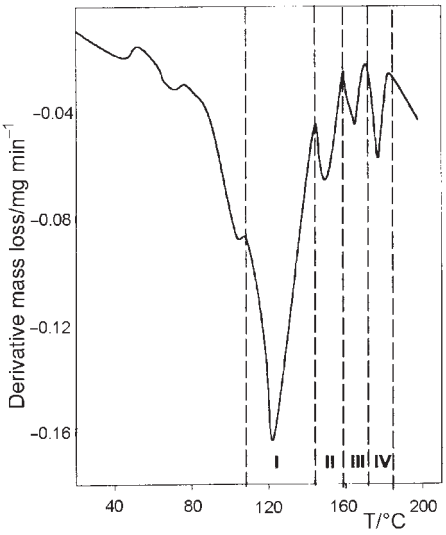

Fig. 5 The Q-DTG curve of *n*-octane thermodesorption from Hg-1223 surface

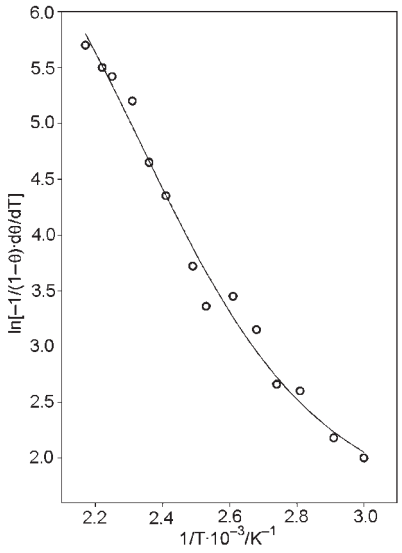

Fig. 6 Plot of the dependence $\ln\left[-\frac{1}{(1-\theta)}\frac{d\theta}{dT}\right] = f\left(\frac{1}{T}\right)$ (Eq. 5) for *n*-octane thermodesorption from the sample surface

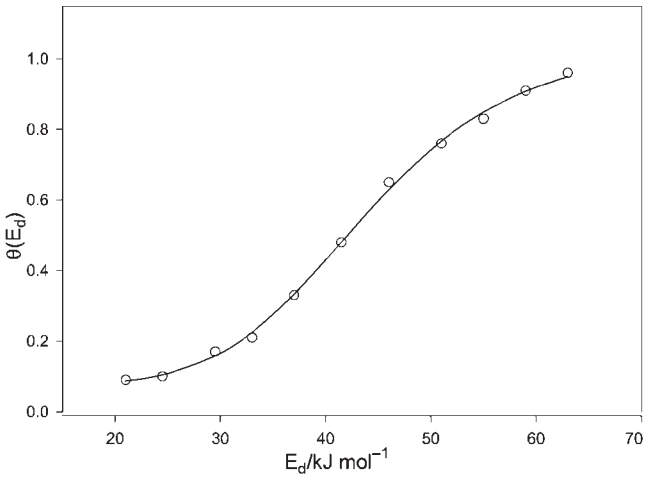

Fig. 7 Plot of the dependence of degree of coverage $\theta(E_d)$ as a function of the desorption energy E_d

with the surface of superconductive material in the adsorption layer. The comparable parameters *N*, for temperature ranges III and IV, correspond practically to the same linearity. Since the desorption energy distribution obtained for range III are comparable with the functions of energy distribution calculated for range IV, they are not presented in this paper. The obtained distribution functions presented in Figs 8–11 are similar to the Weibull distribution function which can be calculated from the equation:

$$\varphi_n(E)=\alpha\lambda E^{\alpha-1}\exp^{-\lambda E^{\alpha}} \tag{17}$$

where α and λ are the distribution parameters.

Table 1 The distribution parameters calculated for all temperature ranges under consideration and values of the desorption energy, *ME*, calculated from Eq. (18)

	T/°C	α	λ	E^{α}_{max}/kJ mol^{-1}	*ME*/kJ mol^{-1}
Total	50–180	4.55	$4\cdot10^{-8}$	40	38.6
I	110–140	6.15	$1.4\cdot10^{-10}$	40	37.6
II	140–160	25	$1.2\cdot10^{-43}$	52	50.6
III	160–170	33.5	$1.46\cdot10^{-57}$	57	55.8
IV	170–180	39.5	$1.56\cdot10^{-71}$	61.5	61.0

Table 1 presents the distribution parameters calculated for all temperature ranges under consideration. Table 1 includes also the values of the desorption energy, *ME*, calculated from equation:

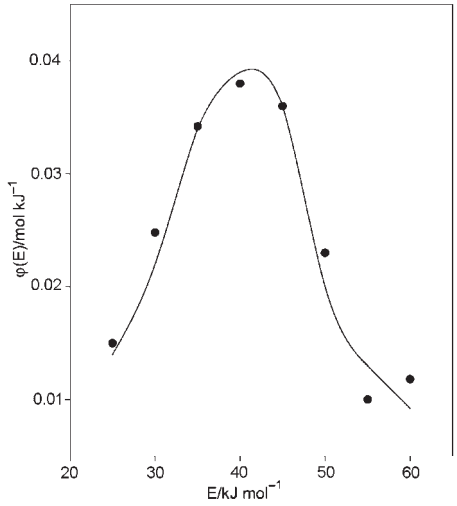

Fig. 8 Energy distribution of *n*-octane desorption from the Hg-1223 surface calculated for the whole temperature range 50–180°C

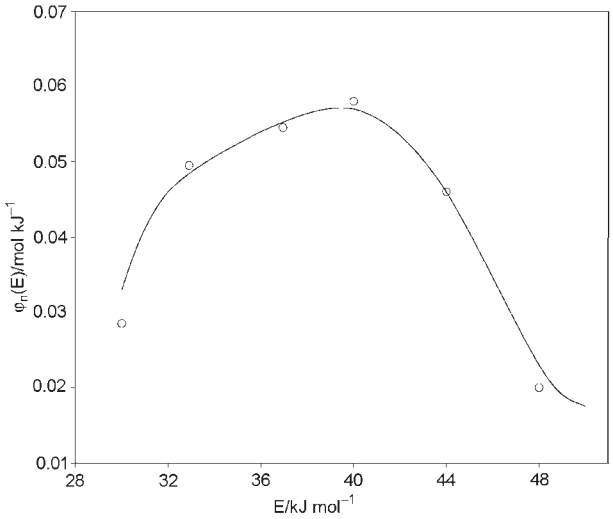

Fig. 9 Energy distribution of *n*-octane desorption from the Hg-1223 surface calculated for the first part of the Q-DTG curve, from 110 to 140°C

$$ME = \lambda^{-\frac{1}{\alpha}} \Gamma\left(\frac{1}{\alpha} + 1\right) \tag{18}$$

where Γ is parameter that characterises the density of the power centres on the given site of a surface.

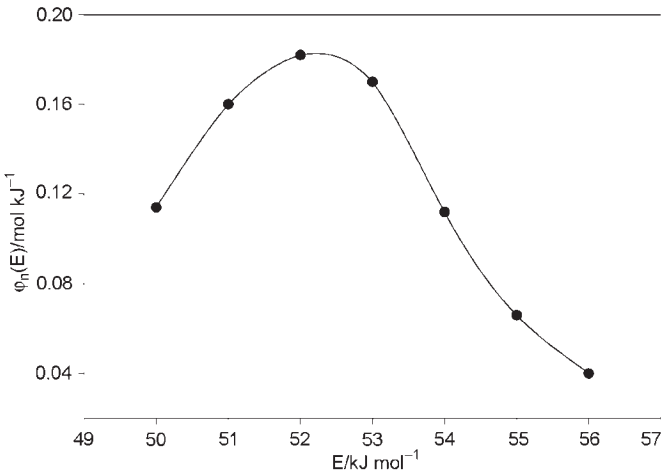

Fig. 10 Energy distribution of *n*-octane desorption from the Hg-1223 surface calculated for the second part of the Q-DTG curve, from 140 to 160°C

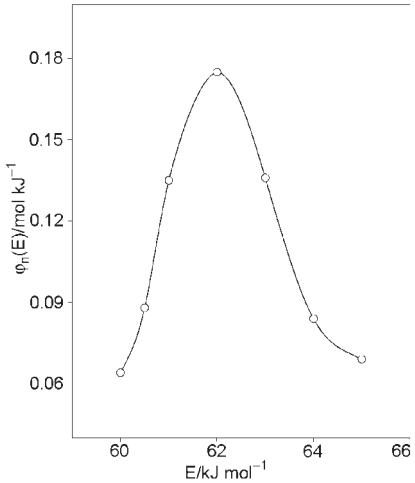

Fig. 11 Energy distribution of *n*-octane desorption from the Hg-1223 surface calculated for the third part of the Q-DTG curve, from 170 to 180°C

As follows from the above Table the calculated values of the desorption energy, *ME*, from Eq. (18), for individual ranges are comparable with the energies, E_{max}^{α}, calculated from Eq. (17). Figures 12a and 12b present the linear dependences of the Weibull distribution parameters α and λ on the desorption energy E_{max}^{α} for each considered temperature range of *n*-octane desorption. In the case of large value of parameter α and small value of λ the calculated distribution functions in Fig. 11 are characterised by a high and narrow peak. This results from the fact that the energy of *n*-octane molecules interaction with the superconductor surface (adsorption centre energy) is greater than that of interaction between *n*-octane molecules.

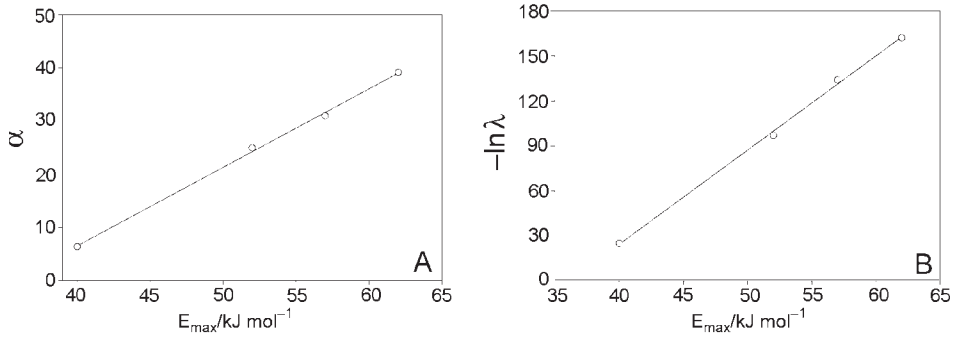

Fig. 12 Plot of dependences of the Weibull distribution parameters, α (A) and λ (B), on the desorption energy, E^{α}_{max} for each considered temperature range of *n*-octane desorption

Conclusions

The presented theoretical and experimental studies demonstrate the possibility of using liquid thermodesorption for determination of the energetic heterogeneity of the adsorbent and material surfaces. Liquid thermodesorption under quasi-isothermal conditions depends on the adsorbate-adsorbate and adsorbate-adsorbent interaction. This special technique of thermal analysis can be successfully applied for studies of solid surface heterogeneity including nonporous adsorbents like high-temperature superconductors. The results presented indicate clearly that the surface of the $HgBa_2Ca_2Cu_3O_{8+\delta}$ sample is energetically heterogeneous. In the range of micro- and mesopores the energy of *n*-octane desorption changes from 28–60 kJ mol^{-1}.

* * *

Thanks are given to Prof. Z. Korczak and Dr. A. Rysak from Department of Experimental Physics, M. Curie-Skłodowska University, Lublin (Poland) for sample studied.

References

1 S. I. Gregg and K. S. Sing, Adsorption, Surface Area and Porosity, 2nd ed., Academic Press, New York 1982.
2 W. Rudziński and D. H. Everett, Adsorption of Gases on Heterogeneous Surfaces, Academic Press, New York 1992.
3 S. Ross and J. P. Olivier, On Physical Adsorption, Interscience, New York 1964.
4 T. L. Hill, J. Chem. Phys., 17 (762) 1949.
5 V. I. Bogillo and P. Staszczuk, J. Therm. Anal. Cal., 55 (1999) 493.
6 P. A. Redhead, Vacuum, 12 (1962) 203.
7 B. Lewis and J. C. Anderson, Nucleation and Growth of Thin Films, New York, Academie Press 1978, p. 325.
8 Y. C. Tovbin and E. V. Vomianov, Russ. J. Fiz. Chem., 67 (1993) 141.
9 V. V. Yashchenko, C. J. Venegas and B. V. Romanovsky, Russ. J. Fiz. Chem., 67 (1993) 1034.

10 Y. C. Tovbin, Russ. J. Phys. Chem., 66 (1992) 1034.
11 V. V. Harlanov, V. I. Bogomalov and N. V. Mirzabienova, Russ. J. Fiz. Chem., (1976) 343.
12 R. C. Boetzold and G. A. Samarjai, J. Catal., 45 (1976) 94.
13 A. Branuer and D. A. Huoul, J. Catal., 56 (1979) 134.
14 J. H. deBoer, Adv. Catal., 8 (1956) 17.
15 J. H. deBoer, The Dynamical Character of Adsorption, Clarendon Press, Oxford 1953.
16 R. Kubo, Statistical Mechanics, North-Holland Publishing Company, Amsterdam 1965, p. 453.
17 V. V. Yashchenko, C. J. Vanegas and B. V. Romanovsky, React. Kinet. and Catal. Letter., 40 (1989) 235.
18 A. Schilling, M. Cantoni, J. D. Guo and H. R. Ott, Nature, 363 (1993) 56.
19 O. Chmaissen, Q. Huang, E. V. Antipov, S. N. Putilin, M. Marezio, S. M. Loureiro, J. J. Capponi, J. L. Tholence and A. Santoro, Physica C, 217 (1993) 265.
20 E. V. Antipov, S. M. Loureiro, C. Chaillout, J. J. Capponi, P. Bordet, J. L. Tholence, S. N. Putilin and M. Marezio, Physica C, 215 (1993) 1.
21 M. Cantoni, A. Schilling, H.-U. Nissen and H. R. Ott, Physica C, 215 (1993) 11.
22 E. K. Isawa, A. Tokiwa-Yamamoto, M. Itoh, S. Adachi and H. Yamauchi, Physica C, 222 (1994) 33.
23 C. W. Chu, L. Gao, F. Chen, Z. J. Huang, R. C. Meng and Y. Y. Xue, Nature, 365 (1993) 323.
24 A. Schilling, O. Jeandupeux, S. Büchi, H. R. Ott and C. Rossel, Physica C, 235 (1994) 229.
25 P. Staszczuk, D. Sternik and G. W. Chądzyński, Congress Journal, Debra J. Bernhardt, Eds, (Published by The Royal Australian Chemical Institute), World Chemistry Congress, Brisbane, Australia 2001, p. 273.
26 P. Staszczuk, J. Therm. Anal. Cal., 53 (1998) 597.
27 F. Paulik, Special Trends in Thermal Analysis, J. Wiley and Sons, Chichester, 1995.